

Neutrino flux ratios at neutrino telescopes: The role of uncertainties of neutrino mixing parameters and applications to neutrino decay

DAVIDE MELONI^{1,*} AND TOMMY OHLSSON^{2,†}

¹*INFN, Sezione di Roma and Dipartimento di Fisica, Università “La Sapienza”,
IT-00185 Rome, Italy*

²*Department of Theoretical Physics, School of Engineering Sciences,
Royal Institute of Technology (KTH) – AlbaNova University Center,
Roslagstullsbacken 21, SE-106 91 Stockholm, Sweden*

Abstract

In this paper, we derive simple and general perturbative formulas for the flavor flux ratios $R_{\alpha\beta} = \phi_{\nu_\alpha}/\phi_{\nu_\beta}$ that could be measured at neutrino telescopes. We discuss in detail the role of the uncertainties of the neutrino mixing parameters showing that they have to be seriously taken into account in any realistic discussion about flavor measurements at neutrino telescopes. In addition, we analyze the impact of such uncertainties in telling the standard neutrino oscillation framework from scenarios involving, *e.g.*, neutrino decay and we find that the ratio $R_{e\mu}$ is the most sensitive one to “new physics” effects beyond the Standard Model. We also compute the more realistic muon-to-shower ratio for a particular configuration of the IceCube experiment, observing that using this experimental quantity a clear separation between standard and non-standard neutrino physics cannot be obtained.

1 Introduction

The standard framework of neutrino oscillations is a successful description of data from recent neutrino experiments. However, there might be subleading effects that are not covered by neutrino oscillations, since the experimental data are still impaired by rather large uncertainties. Such subleading effects could be described by introducing an extended neutrino oscillation framework including so-called damping effects that could stem from, *e.g.*, neutrino decay or neutrino decoherence. In this work, we will introduce damping factors, describing the damping effects, in a phenomenological way as additional factors to the ordinary terms in the formulas for the neutrino oscillation probabilities. A promising situation to look for such subleading effects would be from neutrino sources at large distances, since in this case the result of the damping factors will be most visible because of averaging. In addition, it could be an alternative way to measure the fundamental neutrino parameters, but not the neutrino mass-squared difference, since the averaged neutrino oscillation

*Email: meloni@roma1.infn.it

†Email: tommy@theophys.kth.se

probabilities do not depend on them. Therefore, we will investigate neutrino oscillations with damping effects in general, and different scenarios in which damping effects arise from neutrino decay in particular. We will study these scenarios in the case of neutrinos coming from large distances. The most plausible way to measure such neutrinos would be at neutrino telescopes in ice [1] or water [2]. Many papers in the literature have been devoted to study the dependence of the neutrino fluxes on the neutrino mixing parameters, namely the three leptonic mixing angles θ_{12} , θ_{13} , and θ_{23} as well as the CP-violating phase δ (for an incomplete list of references, see Refs. [3–8]). The usual starting point is that neutrinos are produced via decays of pions and kaons created by hadronic (*i.e.*, pp collisions) and photohadronic ($p\gamma$) interactions [9], leading to the well-known flux ratios at the source $\phi_{\nu_e}^0 : \phi_{\nu_\mu}^0 : \phi_{\nu_\tau}^0 = 1 : 2 : 0$. However, other effects, like muon energy loss in strong magnetic fields [10, 11] can noticeably alter the flavor composition; in addition, a different flux ratio at the source can be obtained for the so-called “neutron beam sources” in which neutrinos are produced from neutron decays [12, 13]. In any case, on their way from the source to the Earth, neutrinos oscillate and the fluxes arriving at the detector acquire a dependence on the neutrino mixing parameters which can, in principle, be used to improve our knowledge on the fundamental neutrino parameters and/or used in connection with reactor experiments and neutrino beams to better the determination of δ and the neutrino mass hierarchy [14]. However, it could happen at the time when neutrino telescopes will be operational that the uncertainties of the neutrino mixing parameters could be large enough not to be neglected in theoretical estimates of the arriving fluxes. This implies that any possible dependence on the neutrino mixing parameters can be completely hidden, and what is also important, that any *small* deviation from the expected number of neutrinos can simply be the effect of our ignorance about the precise values of the neutrino mixing parameters and not due to any “new physics” effects in large distance neutrino oscillations, as those given, *e.g.*, by neutrino decay [15, 16], breakdown of fundamental symmetries [13, 17–19], or pseudo-Dirac nature of neutrinos [20, 21].

For this reason, in this work, we analyze in some detail the impact of the current neutrino mixing parameter errors on the determination of the fluxes arriving at neutrino telescopes. We explicitly illustrate the dependence on the deviation from the best-fit values of θ_{12} , θ_{13} , and θ_{23} up to second order, in the case that the fluxes at the source are in the ratios $\phi_{\nu_e}^0 : \phi_{\nu_\mu}^0 : \phi_{\nu_\tau}^0 = 1 : 2 : 0$. For comparison, we also show how the fluxes on Earth change if neutrino decay takes place and we discuss whether it is possible to distinguish them from the fluxes computed in the standard neutrino oscillation framework, and to what extent.

Our paper is organized as follows: In Sec. 2, we derive the averaged neutrino oscillation probabilities including damping factors. Next, in Sec. 3, we analyze the three-flavor flux ratios and study the impact of the uncertainties of the fundamental neutrino parameters. Then, in Sec. 4, we investigate the flux ratios with neutrino decay, present the different neutrino decay scenarios, as well as we discuss the possibility to detect the subleading effects at neutrino telescopes. Finally, in Sec. 5, we summarize our work as well as we present our conclusions.

2 Derivation of averaged neutrino oscillation probabilities including damping factors

In general, the neutrino oscillation probabilities in the standard three-flavor framework have the following form:

$$P_{\alpha\beta} = \sum_{i=1}^3 \sum_{j=1}^3 J_{\alpha\beta}^{ij} \exp(-i\Phi_{ij}), \quad (1)$$

where $J_{\alpha\beta}^{ij} = U_{\alpha j} U_{\beta j}^* U_{\alpha i}^* U_{\beta i}$ and $\Phi_{ij} = \Delta m_{ij}^2 L / (2E)$. Here U is the leptonic mixing matrix, $\Delta m_{ij}^2 = m_i^2 - m_j^2$ are the neutrino mass-squared differences, L is the baseline length, and E is the neutrino energy. In the case that the ratio L/E is large, *i.e.*, $L/E \gg 2(\Delta m_{ij}^2)^{-1}$, one obtains in vacuum¹ the following averaged neutrino oscillation probabilities

$$\langle P_{\alpha\beta} \rangle = \sum_{i=1}^3 J_{\alpha\beta}^{ii} = \sum_{i=1}^3 |U_{\alpha i}|^2 |U_{\beta i}|^2. \quad (2)$$

Note that these probabilities depend only on the parameters $J_{\alpha\beta}^{ij}$, where $i = j$, as well as they are independent of the oscillation frequencies, since these have been averaged out to zero for large values of the ratio L/E .

Now, introducing damping factors D_{ij} in Eq. (1), the neutrino oscillation probabilities can be written as

$$\begin{aligned} P_{\alpha\beta} &= \sum_{i=1}^3 \sum_{j=1}^3 D_{ij} J_{\alpha\beta}^{ij} \exp(-i\Phi_{ij}) \\ &= \sum_{i=1}^3 D_{ii} J_{\alpha\beta}^{ii} + 2 \sum_{1 \leq i, j \leq 3} D_{ij} |J_{\alpha\beta}^{ij}| \cos(\Phi_{ij} + \arg J_{\alpha\beta}^{ij}), \end{aligned} \quad (3)$$

where the damping factors are given by

$$D_{ij} = \exp\left(-\alpha_{ij} \frac{|\Delta m_{ij}^2|^\xi L^\beta}{E^\gamma}\right) \quad (4)$$

with α_{ij} being elements in a non-negative damping coefficient matrix. We will assume α_{ij} to be independent of energy. Note that both the oscillation frequencies Φ_{ij} and the damping factors D_{ij} are functions of the baseline length L and the neutrino energy E . The oscillation frequencies are functions of the ratio L/E only, whereas the damping factors are more general functions of the parameters L and E , *i.e.*, $D_{ij} = D_{ij}(L^\beta/E^\gamma)$.

Similarly, as in the averaging procedure above for the standard framework, one can perform an averaging of the neutrino oscillation probabilities including damping factors for large values of the ratio L/E , *i.e.*, $L/E \gg 2(\Delta m_{ij}^2)^{-1}$. Note that it would be unnatural to include damping effects after one has performed averaging. Thus, in the case when $\beta = \gamma$, the damping factors are functions of $(L/E)^\beta$ only, and therefore, the following averaging (with $\ell = L/E$) can be introduced²

$$\langle P_{\alpha\beta} \rangle = \lim_{x \rightarrow \infty} \frac{\int_0^x P_{\alpha\beta}(\ell) d\ell}{\int_0^x d\ell} = \lim_{x \rightarrow \infty} \frac{1}{x} \int_0^x P_{\alpha\beta}(\ell) d\ell. \quad (5)$$

¹Matter effects inside the source can affect the neutrino transition probabilities, see Ref. [22].

²Note that averaging with respect to large distances can be obtained by simply assuming E to be a constant, *i.e.*, by defining $\ell = \frac{1}{E}L$, where E is a constant.

In this work, we will not consider the case when $\beta \neq \gamma$. Partly, because this case has less obvious applications. In general, for an arbitrary value of the parameter β , it is not possible to compute the averaged neutrino oscillation probabilities including damping factors, but it is possible for the cases when $\beta = 1$ and $\beta = 2$, which are the cases that are important for applications to scenarios that could arise in Nature, see Ref. [23].

In the case when $\beta = 1$, we obtain

$$\langle P_{\alpha\beta} \rangle = \lim_{x \rightarrow \infty} \sum_{i=1}^3 \sum_{j=1}^3 \langle D_{ij} \rangle(x) J_{\alpha\beta}^{ij}, \quad (6)$$

where the effective damping factors are given by

$$\langle D_{ij} \rangle(x) = \frac{1 - \exp\left(-i \frac{\Delta m_{ij}^2}{2} x - \alpha_{ij} |\Delta m_{ij}^2|^\xi x\right)}{i \frac{\Delta m_{ij}^2}{2} x + \alpha_{ij} |\Delta m_{ij}^2|^\xi x}, \quad (7)$$

which can be written in a more simpler form as

$$\langle D_{ij} \rangle(x) = \sum_{n=0}^{\infty} \frac{1}{n+1} \frac{(-a_{ij}x)^n}{n!}, \quad (8)$$

where

$$a_{ij} = i \frac{\Delta m_{ij}^2}{2} + \alpha_{ij} |\Delta m_{ij}^2|^\xi. \quad (9)$$

For $\xi \neq 0$, the parameters a_{ij} are in general non-zero if $i \neq j$, and therefore, one finds that $\lim_{x \rightarrow \infty} \langle D_{ij} \rangle(x) = 0$, whereas $a_{ij} = 0$ if $i = j$, which means that $\langle D_{ii} \rangle(x) = 1$, and hence, one regains the formula in Eq. (2). On the other hand, for $\xi = 0$, $a_{ij} = \alpha_{ij} + i \frac{\Delta m_{ij}^2}{2}$ if $i \neq j$, and especially, $a_{ij} = \alpha_{ij}$ if $i = j$. Thus, in the case that $\xi = 0$ and in the limit $x \rightarrow \infty$, we find that $\langle P_{\alpha\beta} \rangle = 0$, since $\lim_{x \rightarrow \infty} \langle D_{ij} \rangle(x) = 0$ for all x if $i \neq j$ and $\lim_{x \rightarrow \infty} \langle D_{ij} \rangle(x) = 0$ if $i \neq j$ and $\alpha_{ij} \neq 0$. However, if $\alpha_{ij} = 0$ for fixed $i = j$, then $\lim_{x \rightarrow \infty} \langle D_{ii} \rangle(x) = 1$. Thus, in the case that $\xi = 0$ and $\alpha_{ii} = 0$ for fixed i , the averaged neutrino oscillation probabilities become

$$\langle P_{\alpha\beta} \rangle = J_{\alpha\beta}^{ii} = |U_{\alpha i}|^2 |U_{\beta i}|^2. \quad (10)$$

In general, if $\alpha_{ii} = 0$ for more than one fixed i , then one obtains

$$\langle P_{\alpha\beta} \rangle = \sum_{i \in N} J_{\alpha\beta}^{ii} = \sum_{i \in N} |U_{\alpha i}|^2 |U_{\beta i}|^2, \quad (11)$$

where N can be any of the sets $\{1, 2\}$, $\{1, 3\}$, $\{2, 3\}$, and $\{1, 2, 3\}$. In the case when $N = \{1, 2, 3\}$, one recovers the standard framework formula in Eq. (2).

Similarly, in the case when $\beta = 2$, we can again write the formula for the averaged neutrino oscillation probabilities including damping factors as in Eq. (6), but now the effective damping factors are given by

$$\begin{aligned} \langle D_{ij} \rangle(x) &= \frac{1}{2k_{ij}x} \sqrt{\pi} \exp\left[-\frac{(\Delta m_{ij}^2)^2}{16\alpha_{ij}k_{ij}^2}\right] \\ &\times \left[\operatorname{erf}\left(k_{ij}x + i \frac{\Delta m_{ij}^2}{4k_{ij}}\right) - i \operatorname{erfi}\left(\frac{\Delta m_{ij}^2}{4k_{ij}}\right) \right], \end{aligned} \quad (12)$$

where $k_{ij} = \sqrt{\alpha_{ij} |\Delta m_{ij}^2|^\xi}$. Note that the argument of the imaginary error function is independent of x . Again, the situation is the same as in the case when $\beta = 1$, which means that non-zero averaged neutrino oscillation probabilities can only be obtained for $\xi = 0$ and $\alpha_{ii} = 0$ for fixed i .

3 Neutrino flux ratios

In the cases $\beta = \gamma = 1$ and $\beta = \gamma = 2$, the averaged neutrino oscillation probabilities with damping factors included that are described in Eq. (11) can effectively be written as

$$\langle P_{\alpha\beta} \rangle = \sum_{i=1}^3 d_i J_{\alpha\beta}^{ii}, \quad (13)$$

where d_i are the normalized damping factors, which can have the value 0 or 1. Of course, if $d_i = 1$ for $i = 1, 2, 3$, then one finds the averaged neutrino oscillation probabilities in the standard framework, which are given in Eq. (2).

Starting from the flux ratios at the source $\phi_{\nu_e}^0 : \phi_{\nu_\mu}^0 : \phi_{\nu_\tau}^0 = 1 : 2 : 0$, the neutrino fluxes arriving at a detector are sensitive to neutrino oscillation in vacuum and are then computed as

$$\begin{aligned} \phi_{\nu_e} &= \langle P_{ee} \rangle + 2 \langle P_{\mu e} \rangle, \\ \phi_{\nu_\mu} &= \langle P_{e\mu} \rangle + 2 \langle P_{\mu\mu} \rangle, \\ \phi_{\nu_\tau} &= \langle P_{e\tau} \rangle + 2 \langle P_{\mu\tau} \rangle. \end{aligned} \quad (14)$$

Then, the three-flavor flux ratios analyzed in this work are defined as follows:

$$R_{e\mu} = \frac{\phi_{\nu_e}}{\phi_{\nu_\mu}}, \quad R_{e\tau} = \frac{\phi_{\nu_e}}{\phi_{\nu_\tau}}, \quad R_{\mu\tau} = \frac{\phi_{\nu_\mu}}{\phi_{\nu_\tau}}. \quad (15)$$

3.1 Standard neutrino framework

In this subsection, we analyze the analytical form of three-flavor flux ratios on Earth. These ratios depend on three mixing angles and one CP-violating phase, as implied by Eq. (14), and are, in principle, sensitive to subleading effects (encoded in the dependence of θ_{13}) and the errors of the mixing angles θ_{12} and θ_{23} . For maximal mixing of θ_{23} , *i.e.*, $\theta_{23} = \pi/4$, and vanishing θ_{13} , the robust prediction of Eq. (14) is $\phi_{\nu_e} : \phi_{\nu_\mu} : \phi_{\nu_\tau} = 1 : 1 : 1$ [3], independently of θ_{12} . Going beyond this *zero-order* approximation, allow us not only to study the role of non-maximal θ_{23} and non-vanishing θ_{13} , but also to understand the impact of introducing the uncertainties of the neutrino mixing parameters.

Since the exact formulas for the flux ratios are quite cumbersome, we prefer to present our results in some useful approximations. From experimental data, we know that θ_{13} is small and θ_{23} is close to maximal mixing. For that reason, we can expand the ratios in θ_{13} and $\delta_{23} = \theta_{23} - \pi/4$, parametrizing the deviation from maximal 23-mixing. At the same time, we can also expand for small $\delta_{12} = \theta_{12} - \bar{\theta}_{12}$, $\bar{\theta}_{12}$ being the best-fit value for θ_{12} . No restrictions have been applied on the CP-violating phase δ , which means that the following formulas are valid to all orders in δ . Up to second order in the small quantities θ_{13} , δ_{12} , and δ_{23} , they read

$$\begin{aligned} R_{e\mu} &= 1 + \frac{3}{4} \cos(\delta) \sin(4\theta_{12}) \theta_{13} - \frac{3}{2} \sin^2(2\theta_{12}) \delta_{23} \\ &+ \frac{1}{8} \cos^2(\delta) [3 \cos(4\theta_{12}) - 5] \sin^2(2\theta_{12}) \theta_{13}^2 \\ &+ \frac{1}{32} [-28 \cos(4\theta_{12}) + 3 \cos(8\theta_{12}) - 103] \delta_{23}^2 \\ &+ 3 \cos(\delta) \cos(4\theta_{12}) \delta_{12} \theta_{13} - 3 \sin(4\theta_{12}) \delta_{12} \delta_{23} \end{aligned}$$

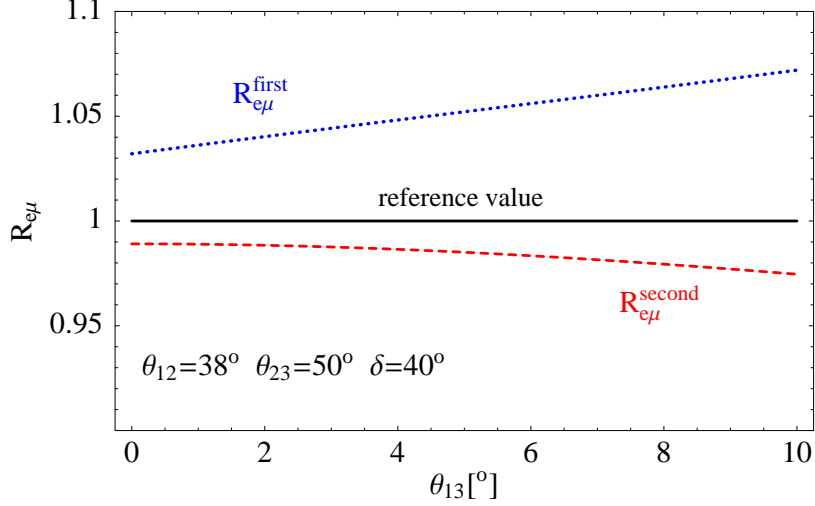


Figure 1: Comparison between the approximate formulas $R_{e\mu}^{\text{first}}$ and $R_{e\mu}^{\text{second}}$ as well as the exact formula for $R_{e\mu}$. The solid curve corresponds to the reference value 1, whereas the dotted and dashed curves correspond to the first- and second-order approximations, respectively.

$$+ \frac{1}{16} \cos(\delta) [3 \sin(8\theta_{12}) - 22 \sin(4\theta_{12})] \theta_{13} \delta_{23}, \quad (16)$$

$$\begin{aligned} R_{e\tau} = & 1 + \frac{3}{4} \cos(\delta) \sin(4\theta_{12}) \theta_{13} - \frac{3}{2} \sin^2(2\theta_{12}) \delta_{23} \\ & + \frac{1}{8} \cos^2(\delta) [3 \cos(4\theta_{12}) + 11] \sin^2(2\theta_{12}) \theta_{13}^2 \\ & + \frac{1}{32} [4 \cos(4\theta_{12}) + 3 \cos(8\theta_{12}) + 121] \delta_{23}^2 \\ & + 3 \cos(\delta) \cos(4\theta_{12}) \delta_{12} \theta_{13} - 3 \sin(4\theta_{12}) \delta_{12} \delta_{23} \\ & + \frac{1}{16} \cos(\delta) [10 \sin(4\theta_{12}) + 3 \sin(8\theta_{12})] \theta_{13} \delta_{23}, \end{aligned} \quad (17)$$

$$\begin{aligned} R_{\mu\tau} = & 1 \\ & + 2 \cos^2(\delta) \sin^2(2\theta_{12}) \theta_{13}^2 + (\cos(4\theta_{12}) + 7) \delta_{23}^2 \\ & + 2 \cos(\delta) \sin(4\theta_{12}) \theta_{13} \delta_{23}. \end{aligned} \quad (18)$$

Now, some comments of the above formulas are in order. First, we discuss the flux ratio $R_{e\mu}$. In Eq. (16), we have clearly separated first- and second-order terms in the series expansion. The approximate relation is obviously much more accurate if referred to small values of θ_{13} , δ_{12} , and δ_{23} . In order to check how good our series expansion is, we show in Fig. 1 the ratio between the approximate formulas (at first and second order, $R_{e\mu}^{\text{first}}$ and $R_{e\mu}^{\text{second}}$, respectively) and the exact formula for $R_{e\mu}$, as a function of the small and unknown mixing angle θ_{13} .

In order to fix some values for the fundamental neutrino parameters, we observe that the following 99 % C.L. limits hold [24]

$$\left\{ \begin{array}{l} 30^\circ < \theta_{12} < 38^\circ \\ 36^\circ < \theta_{23} < 54^\circ \\ 0 < \theta_{13} < 10^\circ \end{array} \right. \quad (19)$$

with best-fit values corresponding to $\bar{\theta}_{12} = 33^\circ$, $\bar{\theta}_{23} = 45^\circ$, and $\bar{\theta}_{13} = 0$. Thus, in order to be sensitive to δ_{12} and δ_{23} , we choose $\theta_{12} = 38^\circ$ and $\theta_{23} = 50^\circ$ (corresponding to $\delta_{12} = \delta_{23} = 5^\circ$).

It can be clearly seen that the second-order approximation reproduces the exact values at the level of 1 % to 3 %, the worst case being obtained for larger values of the mixing angle θ_{13} . The larger discrepancy between the first-order approximation and the reference value is to be mainly ascribed to both the relatively large δ_{23} , which means that second-order terms in this quantity cannot be safely neglected, and the absence of terms of $\mathcal{O}(\delta_{12})$.

At first order in the small parameters, one important feature of this ratio is that it is independent of the error of θ_{12} , which only enter in higher-order terms coupled with the error of the mixing angle θ_{23} . This means that, once you have fixed the value of the mixing angle θ_{12} , its uncertainties are not relevant for the determination of $R_{e\mu}$. Thus, this ratio mainly depends on θ_{13} and the uncertainty of θ_{23} .

In order to estimate which of these parameters encodes the largest part of the uncertainty of $R_{e\mu}$, we can evaluate the maximum spread due to the combination $x = \cos(\delta)\theta_{13}$ ($x = \theta_{23}$) at fixed θ_{23} ($\cos(\delta)\theta_{13}$), namely

$$\Delta R_{e\mu} = \frac{R_{e\mu}(x_{\max}) - R_{e\mu}(x_{\min})}{R_{e\mu}(x = 0)}, \quad (20)$$

$x_{\max, \min}$ being the maximum and minimum value of the variable x . It is simple to derive $\Delta R_{e\mu}$ in the approximations used above. For $x = \cos(\delta)\theta_{13}$, $x_{\max, \min} = \pm\pi/18$ [see Eq. (19)], and for vanishing δ_{12} and δ_{23} , we simply obtain

$$\Delta R_{e\mu} = \frac{\pi}{12} \sin^2(4\theta_{12}) \sim 20 \%, \quad (21)$$

for θ_{12} at the best-fit value. On the other hand, for $x = \delta_{23}$, $x_{\max, \min} = \pm 9\pi/180$, we obtain

$$\Delta R_{e\mu} = \frac{3\pi}{20} \sin^2(2\theta_{12}) \sim 45 \%, \quad (22)$$

which means that the error of θ_{23} contains the largest part of the uncertainty of $R_{e\mu}$.

Then, we discuss the flux ratio $R_{e\tau}$. Due to the approximate $\mu - \tau$ symmetry, the flux ratio $R_{e\tau}$ shares similar characteristics as $R_{e\mu}$, as it can be seen in Eq. (17). In particular, the first-order approximations are exactly the same, whereas differences appear in terms of $\mathcal{O}(\theta_{13}^2)$, $\mathcal{O}(\delta_{23}^2)$, and $\mathcal{O}(\theta_{13}\delta_{23})$.

Finally, we discuss the flux ratio $R_{\mu\tau}$. This flux ratio is very peculiar. At first order in small parameters, it is exactly 1 and the deviation from 1 is only present when second-order terms are included. However, no dependence on the uncertainty δ_{12} is present at least up to $\mathcal{O}(\delta_{12}^2)$, which means that $R_{\mu\tau}$ is mainly sensitive to the central value of the mixing angle θ_{12} , but, once fixed, the uncertainty of it does not affect the flux ratio. What is also an important feature, $R_{\mu\tau}$ is always larger than 1, as it can be seen considering that the terms in Eq. (18) under the conditions in Eq. (19) cannot give negative corrections to 1. This feature is not lost in the exact evaluation, as we have numerically checked. In summary, the flux ratio $R_{\mu\tau}$ is very close to 1, even if the uncertainties of the neutrino mixing parameters are taken into account, since the deviation from its standard value is an effect of second order in small quantities. For that reason, if it could be possible to obtain realistic tau track measurements at neutrino telescopes [see Sec. (4.4)], one could use $R_{\mu\tau}$ as a powerful tool to search for “new physics” effects in neutrino oscillations of high-energy neutrinos.

In order to summarize the previous discussion about uncertainties, we have evaluated the whole spread of the flux ratios $R_{e\mu}$, $R_{e\tau}$, and $R_{\mu\tau}$ due to the present lack of knowledge

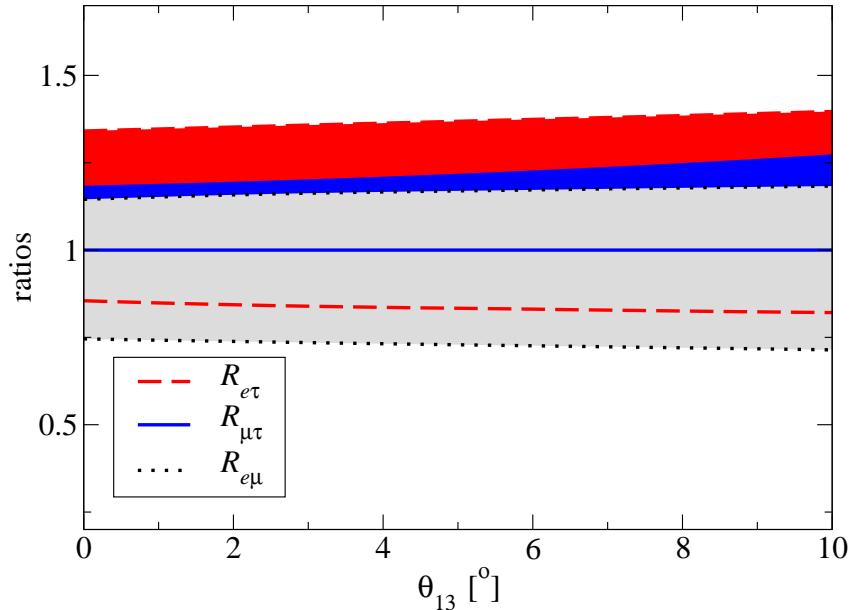


Figure 2: *The spread of the three flux ratios considered in this work due to the present uncertainties of the neutrino mixing parameters as a function of the mixing angle θ_{13} . From above to below: $R_{e\tau}$ (red), $R_{\mu\tau}$ (blue), and $R_{e\mu}$ (grey).*

of the neutrino mixing parameters. We have computed the minimum and maximum values of each $R_{\alpha\beta}$ varying θ_{12} , θ_{23} , and δ in the 99 % C.L. of Eq. (19) and presented the results in Fig. 2 as a function of θ_{13} . From above to below, colored areas contain the possible values for $R_{e\tau}$ (red), $R_{\mu\tau}$ (blue), and $R_{e\mu}$ (grey), respectively. As it can be easily seen, $R_{e\mu}$ can be as large (small) as 1.18 (0.72), whereas $R_{e\tau}$ can assume values ranging from 0.83 to 1.40. On the other hand, $R_{\mu\tau}$ can deviate from unity by 25 %.

Thus, it seems to be clear that even in the case that the flux ratios could be measured with infinite precision at neutrino telescopes, it will be very difficult to estimate or put any reasonable bounds on the neutrino mixing angles (and the CP-violating phase) in the standard three-flavor oscillation framework. In particular, the ratios do not depend in a dramatic way on θ_{13} (both Figs. 1 and 2 numerically confirm this statement) and the dependence on δ is completely overshadowed by the uncertainty of the mixing angle θ_{23} . However, even in the quite unrealistic scenario in which the flux ratio $R_{e\mu}$ will be measured within 5 % precision at future neutrino telescopes and that some long-baseline neutrino experiments gave us a very precise measurement of the mixing angles θ_{12} and θ_{23} (let us say, at the percent level), θ_{13} and δ will not be strongly constrained. In Fig. 3, we quantify this statement showing the allowed pairs (θ_{13}, δ) , which give $R_{e\mu} = 1 \pm 5\%$, for different values of θ_{23} , namely 43° , 45° , and 47° , represented by dotted, solid, and dashed curves, respectively. The admitted parameter space is the region on the left-hand side of the curves. In principle, some values of θ_{13} and δ can be excluded, depending on the assumed value of the mixing angle θ_{23} , but the precision obtained cannot be comparable with that usually claimed for neutrino factories and β -beams.

4 Flux ratios including neutrino decay

Neutrino decay has been invoked in the past to solve both the solar and atmospheric neutrino data problems (see *e.g.* [25–27]). Decay will deplete the flux of neutrinos on

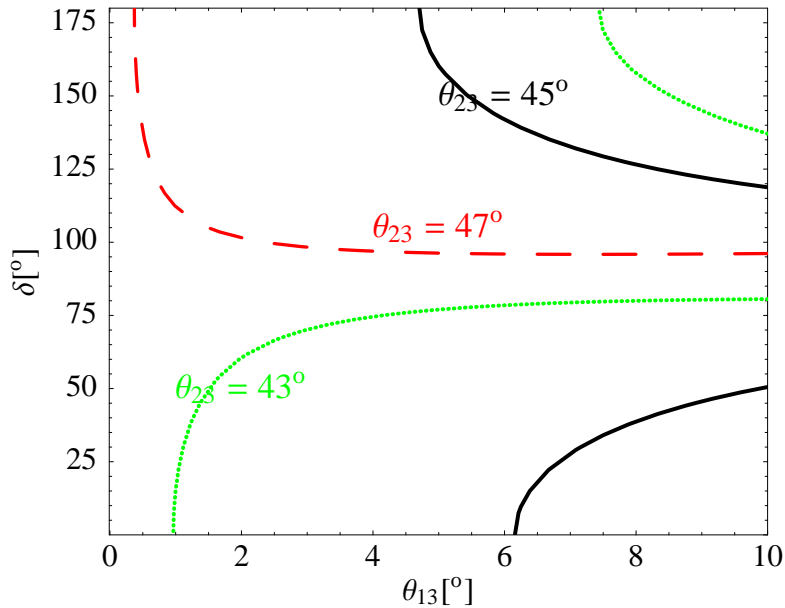


Figure 3: The parameter space giving a value $R_{e\mu} = 1 \pm 5\%$. The dotted, solid, and dashed curves correspond to $\theta_{23} = 43^\circ, 45^\circ, 47^\circ$, respectively. The mixing angle θ_{12} is fixed to 33° .

Earth by the exponential factor

$$\exp\left(-\frac{t}{\tau_{\text{lab}}}\right) = \exp\left(-\frac{L}{E} \frac{m}{\tau}\right) \quad (23)$$

in which τ is the rest-frame neutrino life-time, L the distance between the source and the detector, and E and m are the neutrino energy and mass, respectively. Since neutrino decay scenarios have not been validated so far [28, 29], we can roughly estimate the order of magnitude of the allowed values of the ratio τ/m requiring that $\frac{L}{E} \frac{m}{\tau} \ll 1$. Thus, giving a lower bound $\tau/m \geq 10^{-4}$ s/eV, obtained for a typical L/E solar neutrino [30]. Note that from the supernova SN1987A neutrino events, one would obtain a stronger lower bound at the level of $\tau/m \geq \mathcal{O}(10^5)$ s/eV. However, this bound is not reliable if, as it is the case, the value of θ_{12} is large [31, 32]. Given the bounds previously discussed, we cannot eliminate the possibility of astrophysical neutrino decay. In the following, we will not rely on any specific model for describing the decay process (three-body decays as well as radiative and non-radiative two-body decays have already been discussed in the literature, see *e.g.* Refs. [15, 33] and references therein), but we will assume a pure phenomenological point of view, in which the neutrino completely decay into the lightest mass eigenstates over very large L/E . We adopt here the simplifying assumption that there are no detectable decay products. Two different neutrino decay scenarios (with three active neutrino flavors) will be investigated. In the first scenario, which will be called “neutrino decay I”, the two heaviest neutrino mass eigenstates can decay and only the lightest neutrino mass eigenstate is stable, whereas in the second scenario, which will be called “neutrino decay II”, only the heaviest neutrino mass eigenstate can decay and the two lightest neutrino mass eigenstates are stable. The first neutrino decay scenario, neutrino decay I, has been heavily discussed in the literature, see *e.g.* Ref. [34]. Note that both neutrino decay scenarios can be considered for both normal (NH) and inverted neutrino mass hierarchy (IH), *i.e.*, for the cases, $m_1 < m_2 < m_3$, where m_1 is the mass of the lightest neutrino mass eigenstate, and $m_3 < m_1 < m_2$, where m_3 is the lightest

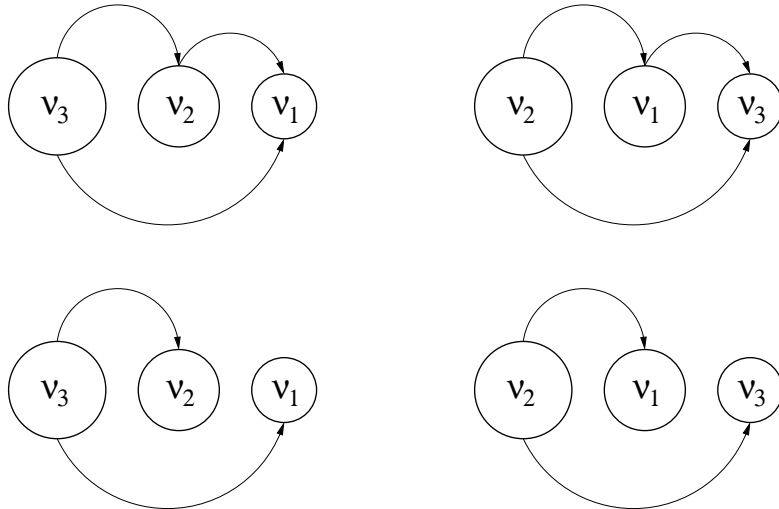


Figure 4: *The two different neutrino decay scenarios. Upper-left picture: Neutrino decay I with normal hierarchy ($\alpha_{11} = 0 \Rightarrow d_1 = 1$). Upper-right picture: Neutrino decay I with inverted hierarchy ($\alpha_{33} = 0 \Rightarrow d_3 = 1$). Lower-left picture: Neutrino decay II with normal hierarchy ($\alpha_{11} = \alpha_{22} = 0 \Rightarrow d_1 = d_2 = 1$). Lower-right picture: Neutrino decay II with inverted hierarchy ($\alpha_{11} = \alpha_{33} = 0 \Rightarrow d_1 = d_3 = 1$).*

neutrino mass eigenstate. The different neutrino decays scenarios are schematically shown in Fig. 4.

In the case of neutrino decay scenarios, the parameter $\beta = 1$, and therefore, we can use Eq. (13) in order to compute averaged neutrino oscillation probabilities (including damping factors). Note that in the case of neutrino decay, the damping coefficient matrix is described by neutrino decay parameters [23], which are defined as $\alpha_{ij} = (\alpha_i + \alpha_j)/2$, where $\alpha_i = m_i/\tau_i$ is the decay rate with m_i being the mass of the i th mass eigenstate and τ_i is its life-time (in its own rest frame) [34]. Thus, in the case of “neutrino decay I”, we have $\alpha_{11} = 0$ or $\alpha_{33} = 0$ and all other α_{ij} ’s are non-zero in general, since only $\alpha_1 = 0$ (NH) or $\alpha_3 = 0$ (IH), which means that $d_1 = 1$ or $d_3 = 1$, *i.e.*, only one of the d_i ’s is equal to 1, and the others are zero (or, in other words, that the exponential factor in Eq. (23) is unity for the lightest mass eigenstate and vanishing for the others). In the case of “neutrino decay II”, we have $\alpha_{11} = \alpha_{22} = 0$ or $\alpha_{11} = \alpha_{33} = 0$, since $\alpha_1 = \alpha_2 = 0$ (NH) or $\alpha_1 = \alpha_3 = 0$ (IH), which means that two of the d_i ’s are different from zero, *i.e.*, $d_1 = d_2 = 1$ or $d_1 = d_3 = 1$. It is now easy to obtain flux ratios on Earth for both scenarios.

4.1 Neutrino decay I

The transition probabilities needed to build the flux ratios for the “neutrino decay I” scenario, illustrated in the first row of Fig. 4, are obtained from Eq. (13) in which the terms $d_i J_{\alpha\beta}^{ii}$ have to be evaluated in the unique index corresponding to the stable mass eigenstate ($i = 1$ for NH and $i = 3$ for IH). The formulas up to the second order in the small parameters θ_{13} , δ_{12} , and δ_{23} are presented in App. A.1. For the sake of simplicity, and with the aim of comparing the neutrino decay scenarios with the standard formulation of large L/E behavior of the flux ratios, we report here only the first-order approximations.³

³In Table 1, the goodness of our approximate formulas can be found.

First, let us discuss the NH case:

$$R_{e\mu} = 2 \cot^2(\theta_{12}) - 4 \cot(\theta_{12}) \csc^2(\theta_{12}) \delta_{12} - 4 \cos(\delta) \cot^3(\theta_{12}) \theta_{13} + 4 \cot^2(\theta_{12}) \delta_{23}, \quad (24)$$

$$R_{e\tau} = 2 \cot^2(\theta_{12}) - 4 \cot(\theta_{12}) \csc^2(\theta_{12}) \delta_{12} + 4 \cos(\delta) \cot^3(\theta_{12}) \theta_{13} - 4 \cot^2(\theta_{12}) \delta_{23}, \quad (25)$$

$$R_{\mu\tau} = 1 + 4 \cos(\delta) \cot(\theta_{12}) \theta_{13} - 4\delta_{23}. \quad (26)$$

The main feature of these formulas are, except for the flux ratio $R_{\mu\tau}$, that the zeroth-order approximation is different from 1, being dependent on $\cot^2(\theta_{12})$. For the best-fit value used in this work, this means that $\phi_{\nu_e} : \phi_{\nu_\mu} : \phi_{\nu_\tau} \sim 5 : 1 : 1$ [16], a very large deviation compared to the standard neutrino framework. Moreover, unlike Eqs. (16) and (17), a dependence on δ_{12} appears at first order, which means that the error of the mixing angle θ_{12} cannot be neglected. Note that $R_{\mu\tau}$ obtains corrections with respect to 1 also at first order. Thus, we expect that the intrinsic uncertainty of the flux ratios (given by our ignorance on the neutrino mixing parameters) is much larger than the standard framework case.

Second, in the case of IH, the flux ratios assume the following simple structure

$$R_{e\mu} = R_{e\tau} = 0, \quad (27)$$

$$R_{\mu\tau} = 1 + 4\delta_{23}. \quad (28)$$

The signature of this particular case is extremely different from both the standard framework and the “neutrino decay I” with NH. Corrections to $R_{e\mu} = 0$ and $R_{e\tau} = 0$ appear at second order in small quantities (see App. A.1) and are dependent on θ_{13} . Thus, we expect a substantial deviation from zero at large θ_{13} , since corrections appear only at second order in θ_{13} [35].

4.2 Neutrino decay II

Similarly, the “neutrino decay II” scenario is depicted in the second row in Fig. 4. In this case, the two lightest neutrino mass eigenstates are stable instead of only the lightest in the “neutrino decay I” scenario. Therefore, we will have two $d_i J_{\alpha\beta}^{ii}$ terms in Eq. (13) instead of only one ($i = 1$ and $i = 2$ for NH and $i = 1$ and $i = 3$ for IH). In App. A.2, we present formulas for the flux ratios only up to first order in the small parameters θ_{13} , δ_{12} , and δ_{23} , since the first-order formulas make a much better approximation for “neutrino decay II” than “neutrino decay I”. Note that for NH, the formulas are independent of δ_{12} . In addition, for both NH and IH, all formulas are dependent on δ_{23} , which means that the uncertainty of θ_{23} is crucial. Furthermore, we observe that the structure of the formulas for NH and IH is very different. For IH, nearly all terms (except from the zeroth-order term of the flux ratio $R_{\mu\tau}$) include the factor $3 - \cos(2\theta_{12}) = 2 + 2\sin^2(\theta_{12})$ in the denominators, which has a value between 2 and 4 and is therefore not equal to zero at any time though. In addition, $R_{e\mu}$ is independent of the CP-violating phase δ , whereas $R_{e\tau}$ is dependent on δ , which actually spoils the approximate $\mu - \tau$ symmetry. In some sense, the values of the flux ratios are closer to the standard neutrino framework for “neutrino decay II” than “neutrino decay I”.⁴

⁴Again, in Table 1, we present the numerical results on the flux ratios.

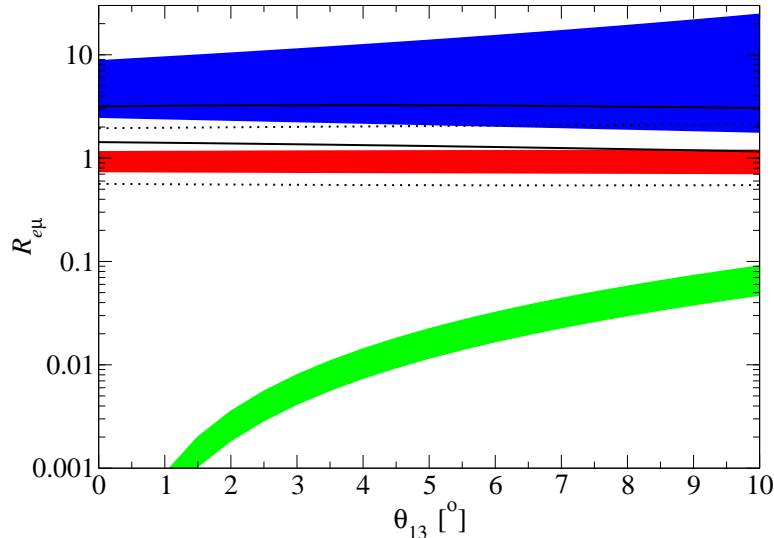


Figure 5: The flux ratio $R_{e\mu}$ including neutrino decay as a function of the mixing angle θ_{13} . The red (middle) area corresponds to the standard neutrino oscillation framework, whereas the blue (upper) and green (lower) areas correspond to neutrino decay with the lightest neutrino mass eigenstate being stable only for NH and IH, respectively. The case of the two lightest neutrino mass eigenstates being stable is visualized by the solid (NH) and dotted (IH) curves, respectively.

4.3 Discussion about the neutrino decay scenarios

The previous considerations have been summarized in Figs. 5 and 6, in which we present the flux ratios $R_{e\mu}$ and $R_{\mu\tau}$, respectively, using the two neutrino decay scenarios with both NH and IH⁵.

In Fig. 5 for the flux ratio $R_{e\mu}$, we observe that the “neutrino decay I” scenario for both NH and IH can, in principle, be distinguished from the standard neutrino oscillation framework. As expected from the very different first-order approximations in Eqs. (24) and (27), even including the errors of the neutrino mixing parameters, the bands representing the total spread of $R_{e\mu}$ are very well separated, especially for the IH case in which the quadratic behavior of θ_{13} predicted in Eq. (45) can be clearly seen (notice that we are using a log scale on the vertical axis). In addition, we observe the large dependence of θ_{13} on the uncertainty of the NH case, which is mainly to be ascribed to the term $4 \cos(\delta) \cot^3(\theta_{12}) \theta_{13}$.

A very different situation arises for the “neutrino decay II” scenario (solid and dotted curves for NH and IH in Fig. 5, respectively). Due to the fact that this scenario contains two stable mass eigenstates, it is quite similar to the standard neutrino oscillation framework, in which all the mass eigenstates are not allowed to decay. Therefore, differences in $R_{e\mu}$ are very difficult to be discerned (the same comment can be applied to Fig. 6).

In Fig. 6, the results of the flux ratio $R_{\mu\tau}$ are shown. As already outlined in the previous section, in the standard framework, $R_{\mu\tau}$ is always larger than 1, even including the uncertainties of the neutrino mixing angles. The neutrino decay scenarios allow $R_{\mu\tau}$

⁵Note that the flux ratio $R_{e\tau}$ is very similar to the flux ratio $R_{e\mu}$, and we have therefore not presented this flux ratio in a separate figure.

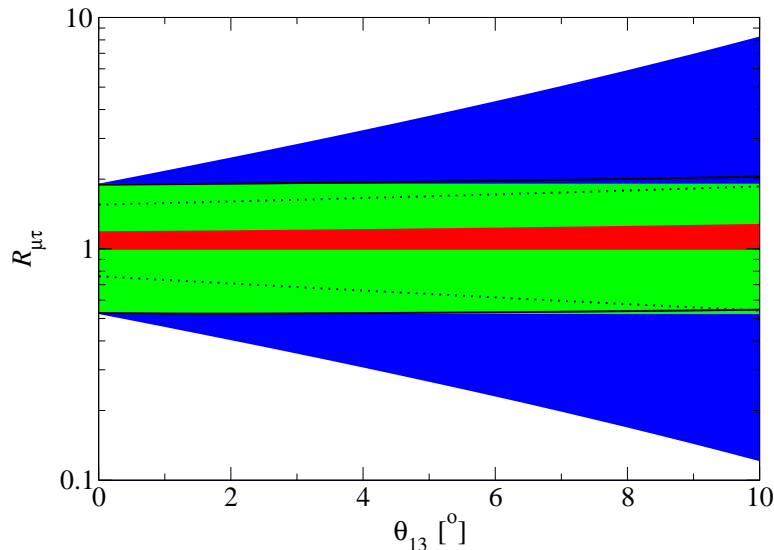


Figure 6: The flux ratio $R_{\mu\tau}$ including neutrino decay as a function of the mixing angle θ_{13} . The red (innermost) area corresponds to the standard neutrino oscillation framework, whereas the blue (outermost) and green (middle) areas correspond to neutrino decay with the lightest neutrino mass eigenstate being stable only for NH and IH, respectively. The case of the two lightest neutrino mass eigenstates being stable is visualized by the solid (NH) and dotted (IH) curves, respectively.

to be smaller than 1 (which could be a clear signature of “new physics” effects), but the large spread of the ratio at any value of θ_{13} does not allow an explicit separation between the standard and decay phenomenologies. Thus, this flux ratio is not a good candidate to find deviations from the standard neutrino oscillation framework.

In Table 1, we present numerical calculations of the flux ratios $\phi_{\nu_e} : \phi_{\nu_\mu} : \phi_{\nu_\tau}$ for the different neutrino decay scenarios, comparing the zeroth-, first-, and second-order results with exact calculations.⁶ In general, we observe that the second-order results contains all the features connected with non-maximal θ_{23} and non-vanishing θ_{13} . Thus, it seems to be important to include second-order effects in any analytical treatment of flux ratios. However, note that the first-order results work especially well for the standard framework and “neutrino decay II”, whereas for “neutrino decay I”, the first-order results do not reproduce all features of the exact computations.

4.4 Discussion about neutrino telescopes

Having discussed the flux ratios from a theoretical point of view, let us now address the question of what can really be measured at neutrino telescopes. The measurement of neutrino flavor seems to be a very difficult task, which means that the three flux ratios previously studied are unlikely to be directly accessible. However, they can be inferred from distinct classes of events: muon tracks, showers, and unique ν_τ signatures (see *e.g.* Ref. [36]). All neutrino flavors undergo neutral-current interactions, which result

⁶Note that the zeroth-order values for the flux ratios in the case of “neutrino decay I” with both NH and IH can, *e.g.*, also be found in Ref. [16].

$\phi_{\nu_e} : \phi_{\nu_\mu} : \phi_{\nu_\tau}$	0 th	1 st	2 nd	exact
standard framework	1:1:1	0.93:1:1	0.93:1.06:1	0.93:1.06:1
neutrino decay I (NH)	4.74:1:1	3.08:1.06:1	3.14:0.99:1	3.20:0.99:1
neutrino decay I (IH)	0:1:1	0:1.35:1	0.02:1.41:1	0.02:1.42:1
neutrino decay II (NH)	2:1:1	1.81:0.65:1	1.78:0.74:1	1.78:0.73:1
neutrino decay II (IH)	1.08:1:1	0.91:1.28:1	0.93:1.30:1	0.93:1.30:1

Table 1: Flux ratios $\phi_{\nu_e} : \phi_{\nu_\mu} : \phi_{\nu_\tau}$ for the different neutrino decay scenarios. 0th, 1st, and 2nd represent the results obtained up to zeroth, first, and second order in small parameters, respectively, whereas the exact computation is given in the column exact. The values of the fundamental neutrino parameters used are: $\theta_{12} = 33^\circ$, $\theta_{13} = 5^\circ$, and $\delta = 40^\circ$. In addition, we have assumed $\delta_{12} = 5^\circ$ and $\delta_{23} = 5^\circ$.

in hadronic showers in a detector. On the other hand, ν_e charged-current interactions also produce electromagnetic showers that, in principle, could be distinguished from the hadronic ones due to the different muon content (which is absent in the electromagnetic showers). However, ν_μ charged-current interactions produce muons always emerging from the shower, which means that this kind of process can be distinguished from a typical shower event, and thus, we do not consider them in the shower rate computation. Finally, the shower rate also includes ν_τ charged-current events, since at least for energies below the order of PeV the tau track cannot be separated from the shower. For energies above the order of PeV, double-bang and lollipop events are also possible, but we do not discuss these tau signatures in this work.

In order to observe a hadronic event inside a telescope, a neutrino must first *survive* as it crosses the atmosphere and then the ice (or water) above the detector. Its typical interaction length in a medium of density ρ is

$$L_0 = \frac{1}{\rho N_A \sigma^{\nu N}}, \quad (29)$$

where $\sigma^{\nu N} = \sigma_{\text{CC}}^{\nu N} + \sigma_{\text{NC}}^{\nu N}$ is the total cross-section to have an interaction that depletes the neutrino energy. It is usual to express this length in terms of its depth: $x_0 = \rho L_0$ (*i.e.*, one meter of water has a depth of 100 g/cm²).

A neutrino from a zenith angle θ_z must cross a column density of material

$$x(\theta_z) = \int_{\theta_z} dl \rho(l, \theta_z). \quad (30)$$

In practice, the path in the atmosphere is negligible and $x(\theta_z)$ is just the depth of the water or ice above the detector. The probability that it does not interact before reaching the detector is then

$$P_{\text{surv}}(E_\nu, \theta_z) = e^{-x/x_0}. \quad (31)$$

Once in the detector, the probability of an event is

$$P_{\text{int}}(E_\nu) \approx 1 - e^{-L\rho N_A \sigma_{\text{int}}^{\nu N}}, \quad (32)$$

where L is the linear dimension of the detector and $\sigma_{\text{int}}^{\nu N}$ is the cross-section for the interaction taken into account (charged or neutral). Therefore, the number of shower events in the telescope in an observation time T for a fixed flavor is

$$N_{\text{sh}} = 2\pi AT \int dE_\nu \frac{d\Phi_{\nu_i}}{dE_\nu} \int d\cos\theta_z P_{\text{surv}} \int_{y_{\text{min}}}^{y_{\text{max}}} dy \frac{1}{\sigma_{\nu N}} \frac{d\sigma_{\nu N}}{dy} P_{\text{int}}, \quad (33)$$

where A is the detector's cross sectional area, $d\Phi_{\nu_i}/dE_\nu$ is the neutrino flux, and θ_z is the zenith angle (in the following, we will consider down-going neutrinos only, which means that tau regeneration effects in matter can be neglected). The variable y is the usual inelasticity parameter in deep-inelastic scattering and represents the fraction of the neutrino energy going into hadronic channels, which means that $E_{\text{sh}} = y E_\nu$.

According to our previous discussion about flavor detectability, for neutral-current interactions and ν_τ charged-currents, we should consider $y_{\text{min}} = y_{\text{thr}} = E_{\text{sh}}^{\text{thr}}/E_\nu$ and $y_{\text{max}} = 1$, where $E_{\text{sh}}^{\text{thr}}$ is the threshold energy for shower detection. For ν_e charged-currents, $y_{\text{min}} = 0$ and $y_{\text{max}} = 1$, since the outgoing electron also shower. Thus, we can evaluate these integrals to obtain the total number of shower events:

$$N_{\text{sh}}^{\text{tot}} = \sum_{\nu_e, \nu_\mu, \nu_\tau} N_{\text{sh}}^{\text{NC}} + \sum_{\nu_e, \nu_\tau} N_{\text{sh}}^{\text{CC}}. \quad (34)$$

Equation (33) is a simple form to evaluate the shower rates at neutrino telescopes. Even if an exhaustive discussion of the problems related to the evaluation of rates is beyond the scope of this work, we should mention two main sources of uncertainties. Obviously, we do not know the neutrino fluxes reaching the Earth's surface, neither the normalization nor the energy behavior. Thus, we can assume the form

$$\frac{d\Phi_{\nu_i}}{dE_\nu} = c \phi_{\nu_i} E_\nu^{-2}, \quad (35)$$

where c is a normalization constant and ϕ_{ν_i} 's are fluxes entering in the definition of the flux ratios in Eq. (15). When calculating the ratios of rates, the normalization factor cancels out, but the spectral index is still a crucial ingredient. In addition, the neutrino-nucleon cross-section is also affected by large uncertainties, mainly due to the extrapolation to very small x required to describe the extremely high-energy regime involved in the processes under discussion.

A high-energy muon undergoes energy loss propagating in the medium, and thus, generating showers along its track by bremsstrahlung, pair production, and photonuclear interactions. These showers are sources of Cherenkov light and can be easily distinguished from showers previously discussed. Equation (33) applies, but now

$$P_{\text{int}}(E_\nu) \approx 1 - e^{-R_\mu \rho N_A \sigma_{\text{int}}^{\nu N}}, \quad (36)$$

where

$$R_\mu = \frac{1}{\beta} \ln \left(\frac{\alpha + \beta E_\mu}{\alpha + \beta E_\mu^{\text{thr}}} \right) \quad (37)$$

with $\alpha = 2 \text{ MeV cm}^2/\text{g}$, $\beta = 4.2 \times 10^{-6} \text{ cm}^2/\text{g}$, $E_\mu = (1 - y) E_\nu$, and E_μ^{thr} is the value of the muon energy to be detected. Note that the y integration in Eq. (33) is modified in such a way that $y_{\text{min}} = 0$ and $y_{\text{max}} = y_{\text{thr}}^\mu = 1 - E_\mu^{\text{thr}}/E_\nu$.

From the previous discussion, it seems to be clear that a viable experimental quantity measurable at neutrino telescopes is the muon tracks N_{tr} to shower ratio. Factorizing out ϕ_{ν_i} from Eq. (35) and calculating the expected rates according to Eq. (33), we obtain

$$\mathcal{R} = \frac{N_{\text{tr}}}{N_{\text{sh}}} = \frac{\phi_{\nu_\mu} N_{\text{tr}}}{\sum_{i=e,\tau} \phi_{\nu_i} (N_{\text{sh},\nu_i}^{\text{CC}} + N_{\text{sh},\nu_i}^{\text{NC}}) + \phi_{\nu_\mu} N_{\text{sh},\nu_\mu}^{\text{NC}}}. \quad (38)$$

Note that the ratio \mathcal{R} depends on the neutrino mixing parameters through the analogous dependence in ϕ_{ν_i} . In order to obtain some clue on the analytical behavior of \mathcal{R} , we can adopt some useful approximations. First of all, we can assume that charged-currents for both neutrino and antineutrino interactions are the same. This is a good approximation above $E_\nu \sim 10^6$ GeV, since at these energies the contribution of valence quarks to the cross-sections is negligible and the νN and $\bar{\nu} N$ cross-sections become equal [37]. In the same energy regime, the charged- and neutral-current cross-sections assume the same functional dependence on the neutrino energy in such a way that

$$R_\sigma = \frac{\sigma_{\text{NC}}}{\sigma_{\text{CC}}} \sim 0.42. \quad (39)$$

It is also a good approximation to assume in Eq. (32) that $L \ll 1/\rho N_A \sigma_{\text{int}}^{\nu N}$ and in Eq. (36) that $R_\mu \ll 1/\rho N_A \sigma_{\text{int}}^{\nu N}$ (the validity of this assumption is expected to be lost at extremely high energies where, in any case, the neutrino flux is very small). Including these approximations in the estimation of the event rate, we can simply express \mathcal{R} in the following way:

$$\mathcal{R} \sim \frac{N_3 \phi_{\nu_\mu}}{N_2 \phi_{\nu_e} + N_1 [R_\sigma (\phi_{\nu_e} + \phi_{\nu_\mu}) + (1 + R_\sigma) \phi_{\nu_\tau}]} \quad (40)$$

in which the numerical constants N_i 's are “remnants” of the full integrals⁷. Now, we can expand in the same small parameters used throughout our work in order to obtain the first-order approximation of Eq. (40). We are interested in the cases of the standard neutrino framework and “neutrino decay I”, since “neutrino decay II” cannot be clearly distinguished from the standard scenario. The complete first-order expansions are also given in App. B. For our discussion, it is enough here to quote their general structure:

$$\begin{aligned} \mathcal{R}^{\text{st}} &= A + B \delta_{23} + C \theta_{13} && \text{(standard framework)} \\ \mathcal{R}^{\text{NH}} &= A' + B' \delta_{23} + C' \theta_{13} + D' \delta_{12} && \text{(neutrino decay I-NH)} \\ \mathcal{R}^{\text{IH}} &= A'' + B'' \delta_{23} && \text{(neutrino decay I-IH)} \end{aligned} \quad (41)$$

in which we have clearly put in evidence of the dependence on the uncertainties δ_{12} and δ_{23} as well as on θ_{13} . The constants A, B, C , and D can be directly read off from the formulas in App. B. From these, we estimate that a partial cancellation of the uncertainties is at work for both \mathcal{R}^{st} and \mathcal{R}^{NH} , whereas a large spread of \mathcal{R}^{IH} could arise due to the current error of θ_{23} . In order to verify these statements, we can use Eq. (38) once the energy thresholds for muons track and shower detection have been specified. To give an example, we use the IceCube detector setup and assume a safe bound of 500 TeV for both types of processes in order to consider event rates well above the atmospheric neutrino backgrounds [38]⁸. For this setup, the result of \mathcal{R} is shown in Fig. 7, in which we have evaluated the whole spread of the muon-to-shower ratio due to the present lack of knowledge of the neutrino mixing parameters, computed with the same strategy used in the other plots (gray bands). We have also included the spread that could be obtained in some years from now after the first new generation of neutrino experiments, assuming a 10 % error of both θ_{12} and θ_{23} (long-dashed curves). Finally, we also included the central value of \mathcal{R} obtained with θ_{12} and θ_{23} fixed to their current best-fit values and $\delta = 0$ (solid curves).

⁷The full expressions for the N_i 's are quoted in App. B.

⁸Note that if we use the Waxman–Bahcall flux [39], we can reproduce the results of Table I in Ref. [38].

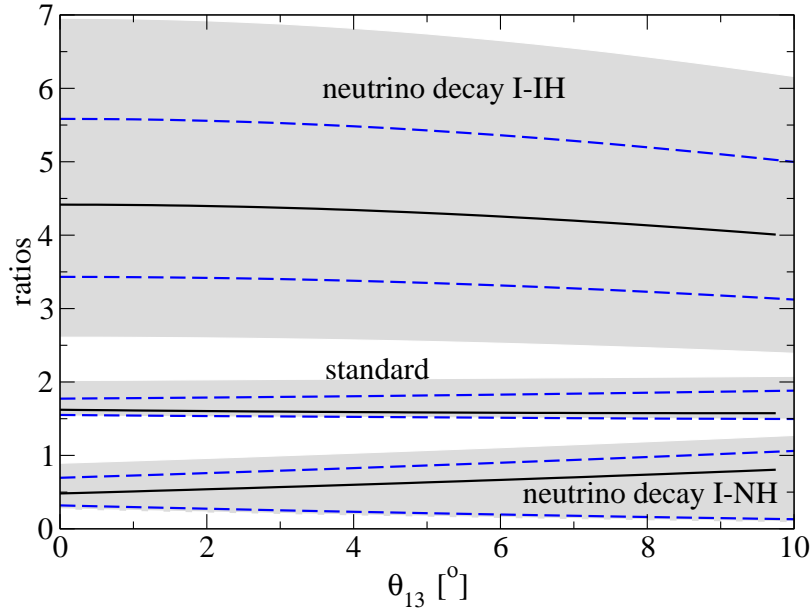


Figure 7: *The muon-to-shower ratio \mathcal{R} as a function of the mixing angle θ_{13} , evaluated for the three scenarios discussed in the main text: standard neutrino framework, neutrino decay I (NH), and neutrino decay I (IH). The bands (the grey-shaded areas) represent the values of \mathcal{R} that can be obtained from the uncertainties of the mixing angles as specified in Eq. (19). The black solid curves inside the bands are the “central” values of \mathcal{R} for the mixing angles θ_{12} and θ_{23} at their best-fit values and $\delta = 0$. The blue long-dashed curves represent the spread that could be obtained assuming a 10 % error of both θ_{12} and θ_{23} .*

We can observe that the three scenarios give different allowed values for \mathcal{R} and also show a mild dependence on θ_{13} . Even if the results obtained keeping θ_{12} and θ_{23} at their best-fit values are clearly separated, the distinction is much less pronounced when including the present uncertainties of the neutrino mixing parameters, and it is unclear if such differences could be distinguished at neutrino telescopes. On the other hand, a reduction of θ_{12} and θ_{23} errors at the level of 10 % improves the situation.

5 Summary and conclusions

The next generation of neutrino telescopes will be able to observe many high-energy events, thus opening the very exciting possibility to measure neutrino flux ratios. However, many uncertainties from both theoretical and experimental point of view, can spoil the capability of extracting useful information about astrophysical sources and fundamental neutrino properties. In this work, we have studied in detail the analytical behavior of the three flux ratios $R_{e\mu}$, $R_{e\tau}$, and $R_{\mu\tau}$, focusing on how the current errors of the neutrino mixing parameters can affect the theoretical expectations of $R_{\alpha\beta}$ for any α and β (for flux ratios at the source $\phi_{\nu_e}^0 : \phi_{\nu_\mu}^0 : \phi_{\nu_\tau}^0 = 1 : 2 : 0$). Due to the enormous distances traveled by neutrinos, the transition probabilities $P_{\alpha\beta}$ among flavors generally assume a simple analytical structure. We have derived them starting from a general treatment of $P_{\alpha\beta}$ which includes damping parameters to account for possible “new physics” effects in neutrino oscillations. We have showed that the only non-vanishing large L averaged transitions are those in which the non-diagonal damping factors completely disappear from the theory. We have then expanded the flux ratios in terms of small parameters, namely the deviation

from maximal θ_{23} , the deviation of θ_{13} from zero, and the deviation of θ_{12} from its best-fit value. Furthermore, we have studied in detail the uncertainties of $R_{\alpha\beta}$ connected with our ignorance of the fundamental neutrino physics. We have observed that the largest indetermination on $R_{e\mu}$ (at the level of 45 %) is due to the fact that we do not know the θ_{23} octant, whereas the uncertainty associated with the product $\cos(\delta)\theta_{13}$ is at least a factor of two smaller. Due to the approximate $\mu-\tau$ symmetry, the same conclusion can be drawn for $R_{e\tau}$. On the other hand, $R_{\mu\tau}$ behaves in a very peculiar way, since the corrections from the standard value $R_{\mu\tau} = 1$ are positive and of $\mathcal{O}(\delta_{12}^2)$. These considerations have been summarized in Fig. 1, in which the total spread of the flux ratios caused by the current uncertainties of mixing parameters seems to be too large to admit the possibility of any realistic measurement of fundamental parameters in the neutrino sector, (*e.g.*, θ_{13} , δ , and the octant of θ_{23}).

We have performed the same detailed study on two different scenarios involving neutrino decay, considering the lightest mass eigenstate (neutrino decay I) or the lightest and next-to-lightest (neutrino decay II) as a stable particle(s). Once the errors of the mixing parameters are included, we have observed that the most promising ratio to measure deviations from the standard framework is $R_{e\mu}$, especially for the “neutrino decay I” scenario with inverted hierarchy. In that case, especially for smaller values of θ_{13} , the difference between the ratios can be as large as two orders of magnitude. On the other hand, the “neutrino decay II” scenario can be hardly distinguished from the standard result.

Finally, we have studied the muon tracks to shower ratio \mathcal{R} at IceCube, as a physical observable directly connected to the experiments. We have evaluated \mathcal{R} in the standard picture of neutrino oscillations and the “neutrino decay I” scenario for both hierarchies. We have found that, contrary to the case in which \mathcal{R} is computed with the neutrino mixing parameters fixed to their best-fit values, the inclusion of parameter uncertainties reduces the possibility to distinguish “new physics” effects in neutrino oscillations. Thus, we believe that any realistic analysis of physics reach of neutrino telescopes concerning flux ratios should carefully include parameters uncertainties.

Acknowledgments

D.M. wishes to thank Paolo Lipari and Olga Mena for very interesting discussions. T.O. would like to thank Evgeny Akhmedov, Mattias Blennow, and Per Olof Hulth for useful discussions. In addition, D.M. would like to thank for the hospitality of the Royal Institute of Technology (KTH) where part of this work was done.

This work was supported by the Royal Swedish Academy of Sciences (KVA), the Swedish Research Council (Vetenskapsrådet), Contract No. 621-2005-3588, and the Magnus Bergvall Foundation.

A Series expansion formulas

A.1 Second-order series expansions of neutrino flux ratios with one non-zero normalized damping factor

The neutrino flux ratios using one of the normalized damping parameters equal to 1, *i.e.*, $d_1 = 1$, and the others equal to zero:

$$\begin{aligned}
 R_{e\mu}(d_1 = 1) &= 2 \cot^2(\theta_{12}) \\
 &\quad - 4 \cot(\theta_{12}) \csc^2(\theta_{12}) \delta_{12} - 4 \cos(\delta) \cot^3(\theta_{12}) \theta_{13} + 4 \cot^2(\theta_{12}) \delta_{23}
 \end{aligned}$$

$$\begin{aligned}
& + 2 [\cos(2\theta_{12}) + 2] \csc^4(\theta_{12}) \delta_{12}^2 \\
& + \{ [4 \cos(2\delta) + 2] \cot^4(\theta_{12}) - 2 \cot^2(\theta_{12}) \} \theta_{13}^2 + 8 \cot^2(\theta_{12}) \delta_{23}^2 \\
& + 12 \cos(\delta) \cot^2(\theta_{12}) \csc^2(\theta_{12}) \delta_{12} \theta_{13} - 8 \cot(\theta_{12}) \csc^2(\theta_{12}) \delta_{12} \delta_{23} \\
& - 16 \cos(\delta) \cot^3(\theta_{12}) \theta_{13} \delta_{23}, \tag{42}
\end{aligned}$$

$$\begin{aligned}
R_{e\tau}(d_1 = 1) & = 2 \cot^2(\theta_{12}) \\
& - 4 \cot(\theta_{12}) \csc^2(\theta_{12}) \delta_{12} + 4 \cos(\delta) \cot^3(\theta_{12}) \theta_{13} - 4 \cot^2(\theta_{12}) \delta_{23} \\
& + 2 [\cos(2\theta_{12}) + 2] \csc^4(\theta_{12}) \delta_{12}^2 \\
& + \{ [4 \cos(2\delta) + 2] \cot^4(\theta_{12}) - 2 \cot^2(\theta_{12}) \} \theta_{13}^2 + 8 \cot^2(\theta_{12}) \delta_{23}^2 \\
& - 12 \cos(\delta) \cot^2(\theta_{12}) \csc^2(\theta_{12}) \delta_{12} \theta_{13} + 8 \cot(\theta_{12}) \csc^2(\theta_{12}) \delta_{12} \delta_{23} \\
& - 16 \cos(\delta) \cot^3(\theta_{12}) \theta_{13} \delta_{23}, \tag{43}
\end{aligned}$$

$$\begin{aligned}
R_{\mu\tau}(d_1 = 1) & = 1 + 4 \cos(\delta) \cot(\theta_{12}) \theta_{13} - 4 \delta_{23} \\
& + 8 \cos^2(\delta) \cot^2(\theta_{12}) \theta_{13}^2 + 8 \delta_{23}^2 \\
& - 4 \cos(\delta) \csc^2(\theta_{12}) \delta_{12} \theta_{13} - 16 \cos(\delta) \cot(\theta_{12}) \theta_{13} \delta_{23}. \tag{44}
\end{aligned}$$

The neutrino flux ratios using one of the normalized damping parameters equal to 1, *i.e.*, $d_3 = 1$, and the others equal to zero:

$$R_{e\mu}(d_3 = 1) = 2\theta_{13}^2, \tag{45}$$

$$R_{e\tau}(d_3 = 1) = 2\theta_{13}^2, \tag{46}$$

$$R_{\mu\tau}(d_3 = 1) = 1 + 4\delta_{23} + 8\delta_{23}^2. \tag{47}$$

A.2 First-order series expansions of neutrino flux ratios with two non-zero normalized damping factors

The neutrino flux ratios using two of the normalized damping parameters equal to 1, *i.e.*, $d_1 = d_2 = 1$, and the last one equal to zero:

$$R_{e\mu}(d_1 = d_2 = 1) = 2 + 2 \cos(\delta) \sin(4\theta_{12}) \theta_{13} + 2[3 + \cos(4\theta_{12})] \delta_{23}, \tag{48}$$

$$R_{e\tau}(d_1 = d_2 = 1) = 2 + 2 \cos(\delta) \sin(4\theta_{12}) \theta_{13} - 4 \sin^2(2\theta_{12}) \delta_{23}, \tag{49}$$

$$R_{\mu\tau}(d_1 = d_2 = 1) = 1 - 4\delta_{23}. \tag{50}$$

The neutrino flux ratios using two of the normalized damping parameters equal to 1, *i.e.*, $d_1 = d_3 = 1$, and the last one equal to zero:

$$R_{e\mu}(d_1 = d_3 = 1) = \frac{4 \cos^2(\theta_{12})}{3 - \cos(2\theta_{12})} - \frac{16 \sin(2\theta_{12})}{[3 - \cos(2\theta_{12})]^2} \delta_{12} - \frac{32 \cos^2(\theta_{12})}{[3 - \cos(2\theta_{12})]^2} \delta_{23}, \tag{51}$$

$$\begin{aligned}
R_{e\tau}(d_1 = d_3 = 1) & = \frac{4 \cos^2(\theta_{12})}{3 - \cos(2\theta_{12})} - \frac{16 \sin(2\theta_{12})}{[3 - \cos(2\theta_{12})]^2} \delta_{12} \\
& + \frac{32 \cos(\delta) \cos^3(\theta_{12}) \sin(\theta_{12})}{[3 - \cos(2\theta_{12})]^2} \theta_{13} - \frac{8 \sin^2(2\theta_{12})}{[3 - \cos(2\theta_{12})]^2} \delta_{23}, \tag{52}
\end{aligned}$$

$$R_{\mu\tau}(d_1 = d_3 = 1) = 1 + \frac{4 \cos(\delta) \sin(2\theta_{12})}{3 - \cos(2\theta_{12})} \theta_{13} + \frac{8 \cos^2(\theta_{12})}{3 - \cos(2\theta_{12})} \delta_{23}. \quad (53)$$

B Expressions for the constants N_1 , N_2 , and N_3 as well as the muon-to-shower ratio

Here, we quote the constants needed to evaluate \mathcal{R} in Eq. (40) using the approximations described in the main text:

$$N_1 = \int dE d \cos \theta_z E_\nu^{-2} P_{\text{surv}}(E_\nu, \theta_z) \int_{y_{\text{thr}}}^1 dy \frac{d\sigma_{CC}}{dy}, \quad (54)$$

$$N_2 = \int dE d \cos \theta_z E_\nu^{-2} P_{\text{surv}}(E_\nu, \theta_z) \sigma_{CC}, \quad (55)$$

$$N_3 = \int dE d \cos \theta_z E_\nu^{-2} P_{\text{surv}}(E_\nu, \theta_z) \int_0^{1-y_{\text{thr}}^\mu} dy \frac{d\sigma_{CC}}{dy} \left(\frac{R_\mu}{L} \right). \quad (56)$$

The first-order expansions of Eq. (40) for the three scenarios considered are the following

- Standard neutrino framework:

$$\mathcal{R}^{\text{st}} = \frac{N_3}{f_1} + \frac{1}{2} f_2 \sin^2(2\theta_{12}) \delta_{23} - \frac{1}{4} f_2 \cos(\delta) \sin(4\theta_{12}) \theta_{13}, \quad (57)$$

where

$$\begin{aligned} f_1 &= N_1 + N_2 + 3N_1 R_\sigma, \\ f_2 &= \frac{3N_3(N_2 + N_1 R_\sigma)}{f_1^2}. \end{aligned}$$

- Neutrino decay I (NH):

$$\begin{aligned} \mathcal{R}^{\text{NH}} &= 2 \frac{N_3 \sin^2(\theta_{12})}{f_1 - (N_1 - 2N_2) \cos(2\theta_{12})} \\ &+ 8 \frac{N_3 (N_2 + N_1 R_\sigma) \sin(2\theta_{12})}{[f_1 - (N_1 - 2N_2) \cos(2\theta_{12})]^2} \delta_{12} \\ &+ 4 \frac{N_3 [f_2 + (N_2 - N_1) \cos(2\theta_{12})] \sin(2\theta_{12})}{[f_1 - (N_1 - 2N_2) \cos(2\theta_{12})]^2} \cos(\delta) \theta_{13} \\ &- 8 \frac{N_3 [f_2 + (N_2 - N_1) \cos(2\theta_{12})] \sin^2(\theta_{12})}{[f_1 - (N_1 - 2N_2) \cos(2\theta_{12})]^2} \delta_{23}, \end{aligned} \quad (58)$$

where

$$\begin{aligned} f_1 &= N_1 + 2N_2 + 4N_1 R_\sigma, \\ f_2 &= N_1 + N_2 + 2N_1 R_\sigma. \end{aligned}$$

- Neutrino decay I (IH):

$$\mathcal{R}^{\text{IH}} = \frac{N_3}{N_1 + 2N_1 R_\sigma} + 4 \frac{N_3 (1 + R_\sigma)}{N_1 (1 + 2R_\sigma)^2} \delta_{23}. \quad (59)$$

References

- [1] A. Achterberg *et al.* (IceCube), *Astropart. Phys.* **26**, 155 (2006), [astro-ph/0604450](#).
- [2] U. F. Katz, *Nucl. Instrum. Meth.* **A567**, 457 (2006), [astro-ph/0606068](#).
- [3] H. Athar, M. Jeżabek, and O. Yasuda, *Phys. Rev.* **D62**, 103007 (2000), [hep-ph/0005104](#).
- [4] P. Bhattacharjee and N. Gupta (2005), [hep-ph/0501191](#).
- [5] P. D. Serpico and M. Kachelrieß, *Phys. Rev. Lett.* **94**, 211102 (2005), [hep-ph/0502088](#).
- [6] P. D. Serpico, *Phys. Rev.* **D73**, 047301 (2006), [hep-ph/0511313](#).
- [7] M. Kachelrieß and R. Tomàs, *Phys. Rev.* **D74**, 063009 (2006), [astro-ph/0606406](#).
- [8] W. Rodejohann (2006), [hep-ph/0612047](#).
- [9] V. L. Ginzburg, V. A. Dogiel, V. S. Berezhinsky, S. V. Bulanov, and V. S. Ptuskin Amsterdam, The Netherlands: North-Holland (1990) 534 p.
- [10] J. P. Rachen and P. Meszaros, *Phys. Rev.* **D58**, 123005 (1998), [astro-ph/9802280](#).
- [11] T. Kashti and E. Waxman, *Phys. Rev. Lett.* **95**, 181101 (2005), [astro-ph/0507599](#).
- [12] L. A. Anchordoqui, H. Goldberg, F. Halzen, and T. J. Weiler, *Phys. Lett.* **B593**, 42 (2004), [astro-ph/0311002](#).
- [13] D. Hooper, D. Morgan, and E. Winstanley, *Phys. Lett.* **B609**, 206 (2005), [hep-ph/0410094](#).
- [14] W. Winter, *Phys. Rev.* **D74**, 033015 (2006), [hep-ph/0604191](#).
- [15] A. Acker, S. Pakvasa, and J. T. Pantaleone, *Phys. Rev.* **D45**, 1 (1992).
- [16] J. F. Beacom, N. F. Bell, D. Hooper, S. Pakvasa, and T. J. Weiler, *Phys. Rev. Lett.* **90**, 181301 (2003), [hep-ph/0211305](#).
- [17] D. Hooper, D. Morgan, and E. Winstanley, *Phys. Rev.* **D72**, 065009 (2005), [hep-ph/0506091](#).
- [18] M. C. Gonzalez-Garcia, F. Halzen, and M. Maltoni, *Phys. Rev.* **D71**, 093010 (2005), [hep-ph/0502223](#).
- [19] L. A. Anchordoqui *et al.*, *Phys. Rev.* **D72**, 065019 (2005), [hep-ph/0506168](#).
- [20] M. Kobayashi and C. S. Lim, *Phys. Rev.* **D64**, 013003 (2001), [hep-ph/0012266](#).
- [21] J. F. Beacom *et al.*, *Phys. Rev. Lett.* **92**, 011101 (2004), [hep-ph/0307151](#).
- [22] O. Mena, I. Mocioiu, and S. Razzaque (2006), [astro-ph/0612325](#).
- [23] M. Blennow, T. Ohlsson, and W. Winter, *JHEP* **06**, 049 (2005), [hep-ph/0502147](#).
- [24] A. Strumia and F. Vissani (2006), [hep-ph/0606054](#).
- [25] S. Pakvasa (1999), [hep-ph/9905426](#).
- [26] P. Lipari and M. Lusignoli, *Phys. Rev.* **D60**, 013003 (1999), [hep-ph/9901350](#).
- [27] V. D. Barger *et al.*, *Phys. Lett.* **B462**, 109 (1999), [hep-ph/9907421](#).
- [28] Y. Ashie *et al.* (Super-Kamiokande), *Phys. Rev. Lett.* **93**, 101801 (2004), [hep-ex/0404034](#).
- [29] T. Araki *et al.* (KamLAND), *Phys. Rev. Lett.* **94**, 081801 (2005), [hep-ex/0406035](#).

- [30] J. F. Beacom and N. F. Bell, Phys. Rev. **D65**, 113009 (2002), [hep-ph/0204111](#).
- [31] J. A. Frieman, H. E. Haber, and K. Freese, Phys. Lett. **B200**, 115 (1988).
- [32] G. L. Fogli, E. Lisi, A. Mirizzi, and D. Montanino, Phys. Rev. **D70**, 013001 (2004), [hep-ph/0401227](#).
- [33] S. Pakvasa, AIP Conf. Proc. **542**, 99 (2000), [hep-ph/0004077](#).
- [34] M. Lindner, T. Ohlsson, and W. Winter, Nucl. Phys. **B607**, 326 (2001), [hep-ph/0103170](#).
- [35] J. F. Beacom, N. F. Bell, D. Hooper, S. Pakvasa, and T. J. Weiler, Phys. Rev. **D69**, 017303 (2004), [hep-ph/0309267](#).
- [36] J. F. Beacom *et al.*, Phys. Rev. D **68**, 093005 (2003), [hep-ph/0307025](#).
- [37] R. Gandhi *et al.*, Phys. Rev. D **58**, 093009 (1998), [hep-ph/9807264](#).
- [38] J. Alvarez-Muñiz *et al.*, Phys. Rev. D **65**, 124015 (2002), [hep-ph/0202081](#).
- [39] E. Waxman and J. Bahcall, Phys. Rev. D **59**, 023002 (1999), [hep-ph/9807282](#).